

# QUANTITATIVE ANALYSIS OF THE SPREADING AND ADHESION OF LATEX BINDER WITHIN PIGMENT COATING LAYER AND ITS RELATION TO THE END-USE PROPERTIES OF THE COATING LAYER

*Jee-Hong Lee<sup>1, 2</sup>, Sang Jin Shin<sup>5</sup>, Seung Uk Yeu<sup>5</sup>  
and Hak Lae Lee<sup>2, 3, 4, \*</sup>*

<sup>1</sup> Center for Coating Materials and Processing, Seoul National University.

<sup>2</sup> Department of Agriculture, Forestry and Bioresources, College of Agriculture and Life Sciences, Seoul National University, South Korea.

<sup>3</sup> Research Institute of Agriculture and Life Sciences, Seoul National University.

<sup>4</sup> State Key Laboratory of Biobased Material and Green Papermaking, Qilu University of Technology (Shandong Academy of Sciences), Jinan, 250353, the People's Republic of China.

<sup>5</sup> Petrochemicals R&D, Research Park, LG Chem. Limited., 34122 Daejeon, South Korea.

## ABSTRACT

The spreading and adhesion behavior of latex is a crucial factor in determining the structure and properties of the low-latex-content pigment coating layer. In spite of its importance, there has been a lack of analytical techniques to describe these characteristics in a coating layer. This study presents novel parameters and techniques for quanti-

\* Corresponding author: lhakl@snu.ac.kr

tative analysis of the spreading and adhesion behavior of latex binder in a coating layer, which is based on cross-section SEM image analysis. A comprehensive series of model coating layers were prepared to achieve varying extents of latex spreading. This was prepared by using latices with different glass transition temperatures and various drying or dry-sintering conditions. Parameters were developed to determine and quantify the different morphological characteristics of latices in the coating layers, which had advantages over qualitative observation from the SEM images. Developed analytical techniques were applied to reveal correlations between structural properties and the coating end-use properties, which contributed to a better understanding of coating structure development. A transitional change in coating structure was observed in the low latex spreading domain and this largely influenced the end-use properties of coating layers such as the mechanical properties and light-scattering efficiency. Micro-roughness of the coating surface and gloss were positively correlated to the spreading extent of the latex. It was notable that despite low levels of coating shrinkage due to the low latex content, the micro-roughness still changed with latex spreading variations. Quantitative analysis of latex spreading and mechanical properties of the coating layer also enabled us to separate the adhesion behavior of latex binder into physical and chemical aspects. This would propose a strategy for paper manufacturers to optimize their coated paper products.

**Key words:** Coating structure, image analysis, spreading of latex, pigment-binder interface, mechanical property

## 1 INTRODUCTION

Pigment coating is often used to improve the end-use properties of paper and paper-board products or to impart special functionalities such as barrier properties. The coating is an aqueous suspension typically consists of inorganic pigments, latex binder, and other additives. Pigment coatings used in the paper industry are mainly characterized by a low binder content which makes pores be introduced into the structure of the dry pigment coating layer. The micro-structure of pigment coating layer has long been recognized for its importance in determining coating properties. In particular, the distribution of constituents by binder migration has received a lot of attention because it greatly influences the various properties of coated paper products [1-4]. The spreading of latex particles is also a crucial factor in determining the properties of coated paper products. This affects the mechanical properties of the

coating layer by determining the coverage of the latex binder on the pigment particles. Furthermore, the deformability of latex significantly influences the consolidation process [5-7], thereby influencing the pore structure and printability [6, 8-10]. Despite their importance, analytical techniques for investigating the spreading and adhesion behavior of latex binders in pigment coating layer are lacking.

Several approaches have been used to investigate the spreading behavior of latex [5, 8, 11-17]. Topographical images of an individual latex particle on a model inorganic surface obtained by atomic force microscopy (AFM) [11-14] or scanning electron microscopy (SEM) [15-16] has been used for quantitative analysis of latex spreading. Although these methods have provided valuable information on the spreading behavior of an individual latex particle, the experimental situation cannot reproduce the actual coating process. This is because these methods excluded the effects such as interactions between the coating constituents and stresses arising during the consolidation process. SEM images have also been used, but only for a qualitative assessment of the spreading of latex at the coating layer surface [5, 8]. Small angle neutron scattering (SANS) technique was used to investigate the ordering and spreading of latex particles in calcium carbonate coatings [17]. However, this approach provided an average spatial information on the aggregation and film formation of latex particles. Although many research efforts have been made to explain the spreading behavior of latex particles, there is a need to evaluate the spreading behavior of latex within the coating layer more systemically and quantitatively.

This study presents novel parameters and techniques for quantitative analysis of the spreading and adhesion behavior of latex binders in pigment coating layers based on SEM cross-sectional image analysis. The developed analytical techniques were applied to coating layers prepared with different  $T_g$  latexes and dried under different drying or dry-sintering conditions. The spreading and adhesion of latex, pore structure, dimension, and surface micro-roughness of the coating layer were evaluated and compared with the coating end-use properties, i.e. surface smoothness, optical properties, and mechanical properties. A novel approach to measure the mechanical properties of coating layers has also been developed and applied. Developed approaches were used to reveal various relationships between the structural properties and end-use properties of coating layers, contributing to a better understanding of the fundamentals of pigment coatings.

## **2 EXPERIMENTAL**

### **2.1 Preparation of coating layers**

Ground calcium carbonate (Setacarb-HG, 98 % < 2  $\mu\text{m}$ , 9 % < 1  $\mu\text{m}$ , top cut = 3  $\mu\text{m}$ , Omya Inc.) was used as a pigment. Four different coating colors were

prepared using four different styrene-butadiene (S/B) latexes (provided by LG Chem. Ltd., Korea) (Table 1). The latexes were prepared to have different glass transition temperatures ( $T_g$ ) but similar in particle size and gel content. The S/B composition of the latex was varied to control  $T_g$ , and the amount of chain transfer agent was varied to ensure similar gel contents in all latices. A constant amount of each latex, 12 parts per hundred per the dry weight of pigment, was used. The coating color consisted of the pigment and a latex binder, without any other additives. The solids content of the coating color was 62% and the pH was controlled to 9.5 with 1N sodium hydroxide (NaOH) solution. Corona treated polyethylene terephthalate (PET) having a thickness of 100  $\mu\text{m}$  was used as a substrate. After applying the coating colors using a laboratory automatic rod coater (GIST, Korea), it was dried using a hot-air drying oven. Some of the coating layers dried at 25°C were heated to different temperatures to induce dry-sintering of the latex particles. Different drying and dry-sintering conditions were applied to the coating layers (Table 2). Some of the coating layers composed of SBL-4 latex was

**Table 1.** Properties of styrene-butadiene latexes.

	$T_g$ , (°C)	MFFT, (°C)	Particle size, (nm)	Gel content, (%)
SBL-1	2.9	0.2	146.2	73.2
SBL-2	11.8	7.6	154.4	77.5
SBL-3	19.3	16.1	151.3	74.2
SBL-4	34.7	30.3	153.2	77.6

MFFT = minimum film-forming temperature

**Table 2.** Drying and dry-sintering conditions for the coating layers.

Latexes used	SBL-1	SBL-2	SBL-3	SBL-4
<b>Drying condition</b>				
25 °C, 3 min	O	O	O	O
60 °C, 2 min	O	O	O	O
120 °C, 2 min	O	O	O	O
<b>Dry-sintering condition</b>	<b>Dried coating layers at 25 °C for more than 3 min. were used in dry-sintering experiments</b>			
60 °C, 15 min	O	O	O	O
120 °C, 15 min	O	O	O	O
60 °C, 30 min	-	-	-	O
120 °C, 30 min	-	-	-	O

exposed to a longer dry-sintering period to determine the influence of duration. The coat weight and thickness of the coating layer was  $10.8 (\pm 0.6) \text{ g/m}^2$  and  $7.7 \pm 0.3 \text{ }\mu\text{m}$ , respectively. After each drying and dry-sintering process, the coating layer samples were conditioned at constant temperature and relative humidity ( $25^\circ\text{C}$ , 50% RH) for more than 24 hours.

## **2.2 Cross-section sample preparation and image acquisition**

Coating layers were stained with osmium tetroxide ( $\text{OsO}_4$ ) and resin-embedded for cross-section imaging. Coating layer samples were cut into  $3 \times 1 \text{ cm}^2$  sections and stained in  $\text{OsO}_4$  vapor for at least 48 hours. Stained samples were embedded in a mixture of epoxy resin (EpoFix Resin, Struers) and hardener for 20 min. Thereafter, the excess mixture was wiped off and the samples were cured at ambient temperature for at least 24 hours. The stained and embedded samples were attached to an SEM stub with a carbon tape and platinum sputtered.

Cross-section images were obtained using FIB-FESEM (Auriga, Carl Zeiss). FIB milling was proceeded in two stages: Coarse milling with a high current ion beam (16 nA) in a trapezoid shape, then fine milling with low current ion beam (1 nA). Milling depth was  $17 \text{ }\mu\text{m}$ . The accelerating voltage was 1.60 kV, and  $20,000\times$  images were obtained for analysis. Both secondary electron (SE) mode and energy selective backscattered electron (EsB) mode images were obtained, and at least 10 pairs of images per each experimental condition were used for analysis. Care was taken to minimize intensity difference between the images. Each step of these processes has been verified in our previous works [18–19].

## **2.3 Image processing and analysis**

### *2.3.1 Spreading and adhesion behavior of latices*

Figures 1 and 2 present the image processing and analysis procedures developed to quantify the spreading and adhesion behavior of the latex binder in a coating layer. Adobe Photoshop CC 2018, MATLAB (The Mathworks, Natick, MA, U.S.A.) and Image J software were used for image processing and analysis. Three novel parameters were proposed. The surface area (S.A.) index, calculated by dividing the square of the perimeter of binder divided by the area of binder, indicates how well the latices are dispersed and spread (Figure 1). This index was derived from the fact that a larger surface area is formed at a given dosage of binder when the binder is well dispersed and spreads more. The calculation assumes that the dosage of binder corresponds to the area of the binder and the surface area of binder corresponds to the perimeter of the binder in a two-dimensional cross-section of the coating layer.

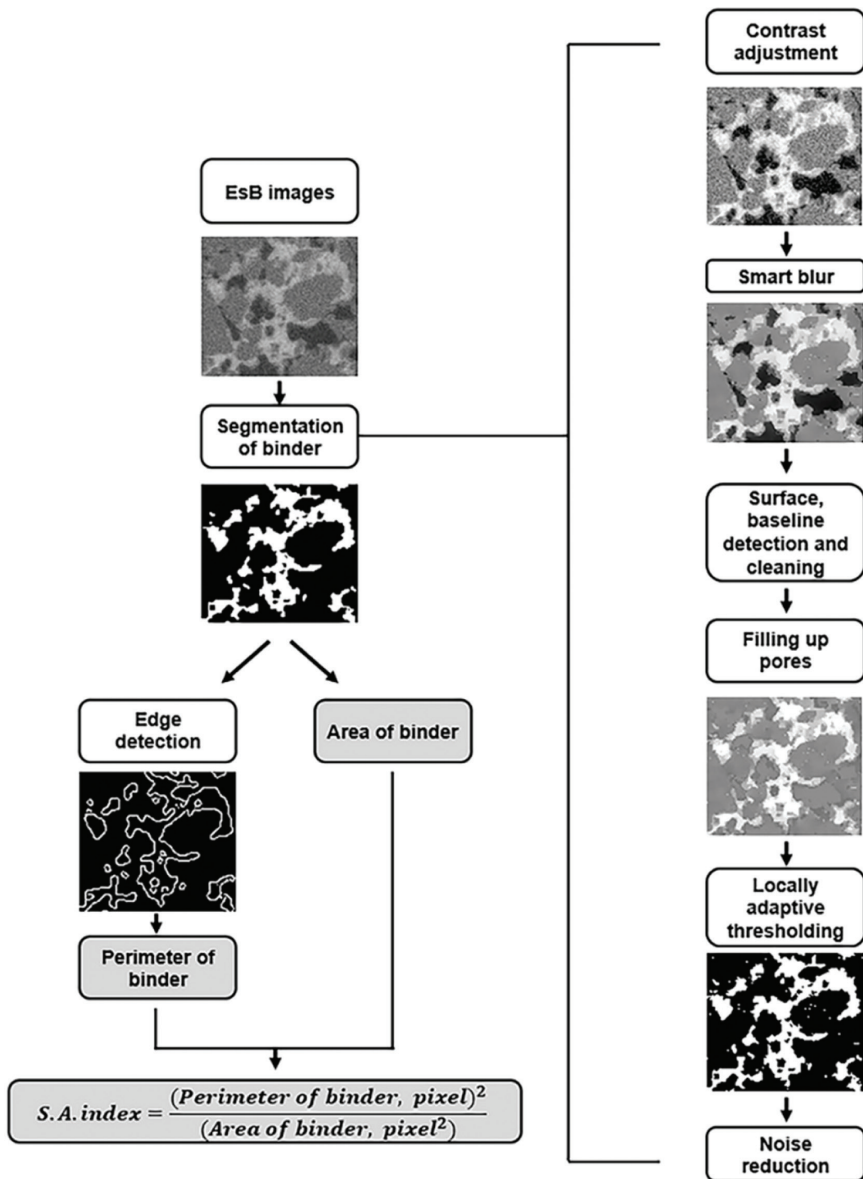
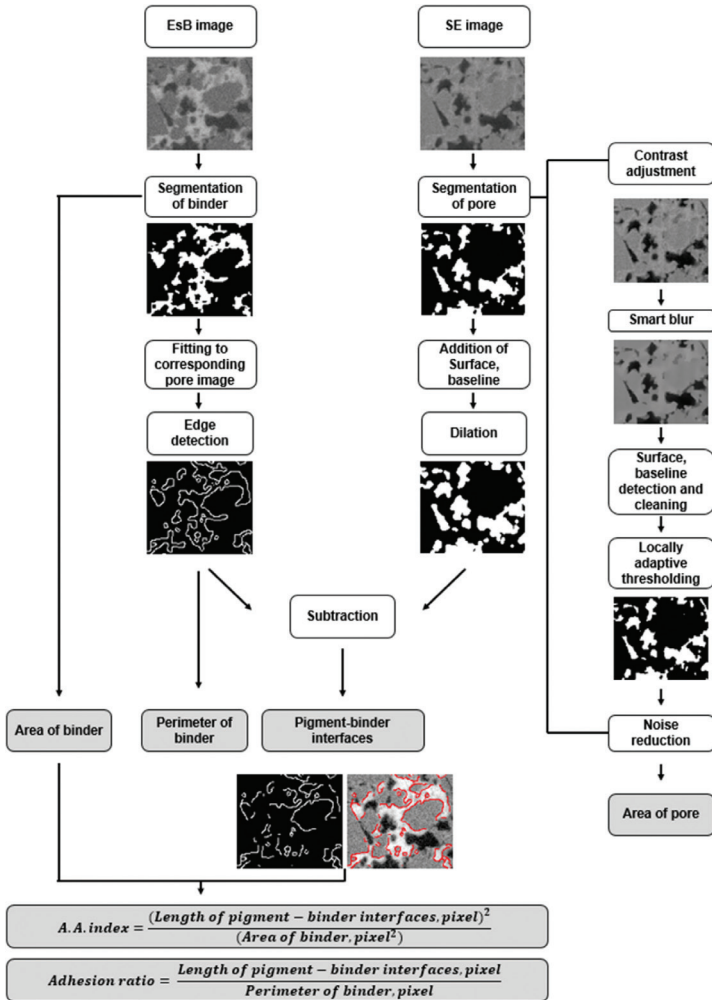


Figure 1. Image processing and analysis procedure for surface area (S.A.) index.

The second parameter, the adhesion area (A.A.) index, indicates how much the binder physically adheres to the pigment at a given binder dosage. This index was calculated as the square of the length of pigment–binder interface divided by the area of binder (Figure 2). The calculation assumes that the length of the pigment–binder interface is the area of adhesion of the binder to the pigment in the two-



**Figure 2.** Image processing and analysis procedure for adhesion area (A.A.) index and adhesion ratio. The red lines in the final image present the segmented pigment–binder interfaces superimposed on the contrast-enhanced EsB image.

dimensional cross-section image. The third parameter, the adhesion ratio, indicates the ratio of the surface area of the binder involved in the adhesion to pigment. This was calculated by dividing the length of the pigment–binder interface by the perimeter of the binder (Figure 2).

The length distribution of the pigment–binder interface was also analyzed. The ratio of the length of the pigment–binder interface summed at a specific length interval to the total length of pigment–binder interface was calculated and plotted as a cumulative graph. This ratio represents the contribution of a specific pigment–binder interface length to the total amount of pigment–binder interface in the coating layer. The length of pigment–binder interface at the median of this ratio was used to represent the distribution.

To obtain these parameters, three measurements were made on the coating layer images: the area of the binder, the perimeter of the binder, and the length of pigment–binder interface. The area and perimeter of the binder was obtained from the segmented binder images. However, additional processing steps were required to obtain the pigment–binder interface. The principle of the image processing procedure to obtain it is presented in Figure 3. Since the image intensity values cannot be negative in the binarized image, the pigment–binder interface can be obtained by subtracting the perimeter of the pore from the perimeter of binder. The image segmentation process for binders and pores developed in our previous studies [18–19] was advantageous for segmentation of the pigment–binder interface because it preserves small targets and the edges of the target. The major features of this segmentation process are smart blur and locally adaptive thresholding techniques.

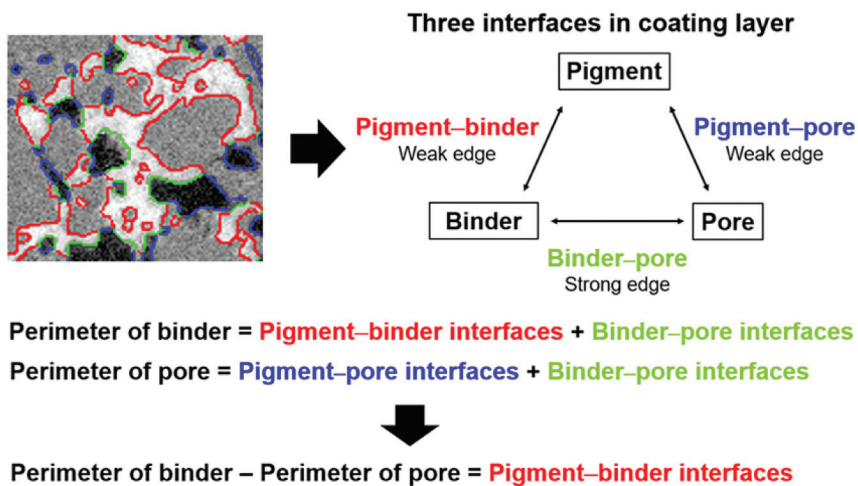


Figure 3. Principle of image processing procedure to obtain pigment–binder interfaces.

### *2.3.2 Pore structure, dimension, and surface micro-roughness*

Pore structure was analyzed using the segmented pores in Figure 2. Porosity was calculated by dividing the segmented pore area by the total area of the coating layer. The pore size distribution was determined as the ratio of the sum of the areas of the pores at a specific interval of pore radius to the total pore area, and displayed as a cumulative graph. This ratio indicates how much the size of pores contributes to the total porosity of the coating. The equivalent radius was calculated to describe the pore radius. The pore radius at the median of this ratio was used to represent the pore size distribution.

The thickness of the coating layer was calculated by dividing the total area of the coating layer by the width of the coating layer. The micro-roughness of the coating surface was presented as the arithmetic mean roughness calculated from the surface profile of the cross-section image (Equation 1). The surface profile was separated and aligned using a linear regression line of the coating layer. Then, the arithmetic mean roughness was calculated. The sampling interval for the roughness calculation was 1 pixel, which corresponds to 13.7 nm.

$$R_a = \frac{1}{l} \int_0^l |z(x)| dx \quad (1)$$

where  $R_a$  = arithmetic mean roughness (nm),  $l$  = width of coating layer (nm),  $z$  = deviation of profile from the mean line (nm).

## **2.4 Measurement of the end-use properties of coating layers**

### *2.4.1 A novel approach to measure the mechanical property of coating layers*

A SAICAS (Daipia Wintes, Japan) instrument was used to measure the mechanical properties of the coating layer. Compared to the conventional method, this method has the advantages of (1) failure to occur only near the cutting blade, thereby excluding the adhesion effect between the coating–substrate interface, and (2) not requiring any special sample preparation process. An analysis of the sectioned area was performed to determine whether this method gave reliable results. The tilted FESEM images showed no direct slicing of the pigment particles, suggesting that the failure occurred within the binder or at the pigment–binder interface (Figure 4). Reports have shown that the adhesion failure is dominant over cohesive failure [20–22], indicating that the failure mainly occurs at the pigment–binder interface. Depth measurement was performed with coating layers prepared with eight representative experimental conditions that include the highest and lowest mechanical strengths. The results confirmed that the instrument provided

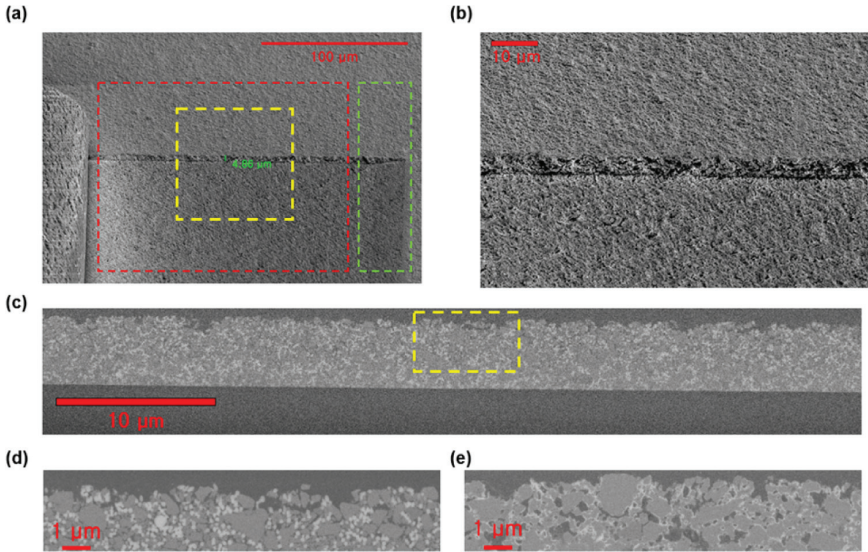


**Figure 4.** SEM images of the coating fractured by SAICAS measurement. (a) Tilted top-view SEM image, green rectangle: cutting stage, red rectangle: peeling stage, (b) magnified image of the yellow rectangle in (a), (c) cross-section of a sectioned area in the peeling stage (non-filming latex), (d) magnified image of the yellow rectangle in (c). (e) Cross-section of a sectioned area in the peeling stage (filming latex). Note that (d) shows the coating layer composed of SBL-4 dried at 25 °C, and (e) shows the coating layer composed of SBL-1 dried at 25 °C.

uniform and reproducible sectioning of the coating layer regardless of the mechanical strength of the coating layer [23].

The SAICAS measurement process was proceeded in two stages (Figure 5). In the cutting stage, a diamond cutting blade with a rake angle of 40° was inserted through the coating layer at a horizontal velocity of 0.8 μm/s and a vertical velocity of 0.08 μm/s. In the peeling stage, the blade moves horizontally at a velocity of 0.8 μm/s through the coating layer. The peel strength was calculated using the load data obtained from the peeling stage at 30 – 120 s (Equation 2). At least 5 measurements were made for each sample.

$$P = \frac{F_{HAve}}{w} \quad (2)$$

where P is the peel strength (N m<sup>-1</sup>),  $F_{HAve}$  is the average horizontal load (N), and w is the blade width. (m).

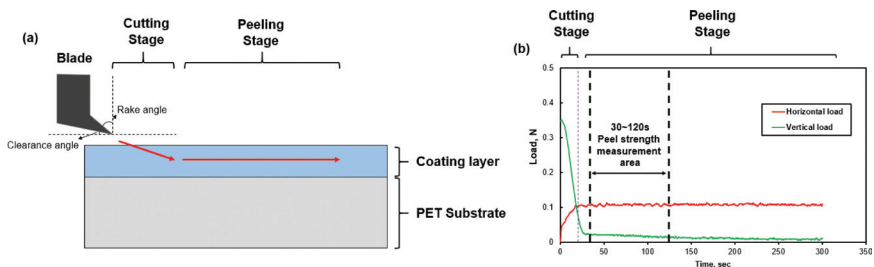


**Figure 5.** Description of SAICAS measurement process. (a) A schematic view of the measurement process, (b) a graph of representative results of the measurement.

#### 2.4.2 Surface and optical properties

Gloss, Parker Print-Surf (PPS) roughness, and light-scattering efficiency of the coating layers were measured. Gloss was determined using a gloss meter (Lorentzen & Wettre, L&W) according to TAPPI T 480 Gloss (75°). PPS roughness was measured using a PPS tester (L&W). Light-scattering efficiency was measured using an L&W Elrepho instrument. The reflectance of the coating layers was measured against black-and-white backgrounds. The light-scattering coefficient was determined according to ISO 9416.

### 3 RESULTS AND DISCUSSION

#### 3.1 Qualitative vs Quantitative

The coating layer images in Figure 6 show that the morphological change in the latex binder depends on the  $T_g$  of latex used and the processing conditions. Using a lower  $T_g$  binder or increasing the processing temperature changed the shape of the latex particles from spherical to thin film-like one, yielding a “channel-like” structure with extensive connectivity. Binder particles with the deformed structures covered a larger surface area of the pigment particles. Particularly, it was noticeable that small pigment particles were almost completely covered by the binder.

The direct observation via SEM images allowed a qualitative evaluation of the spreading and adhesion behavior of binders. However, this was applicable when there was a significant difference. In many cases, visual observation does not provide a clear comparison between samples. For instance, when the drying temperature was increased from 25 °C to 60 °C, the morphological change of the binder particles was discernible in the SBL-4 coating layer, but not in the SBL-1, SBL-2 and SBL-3 coating layers.

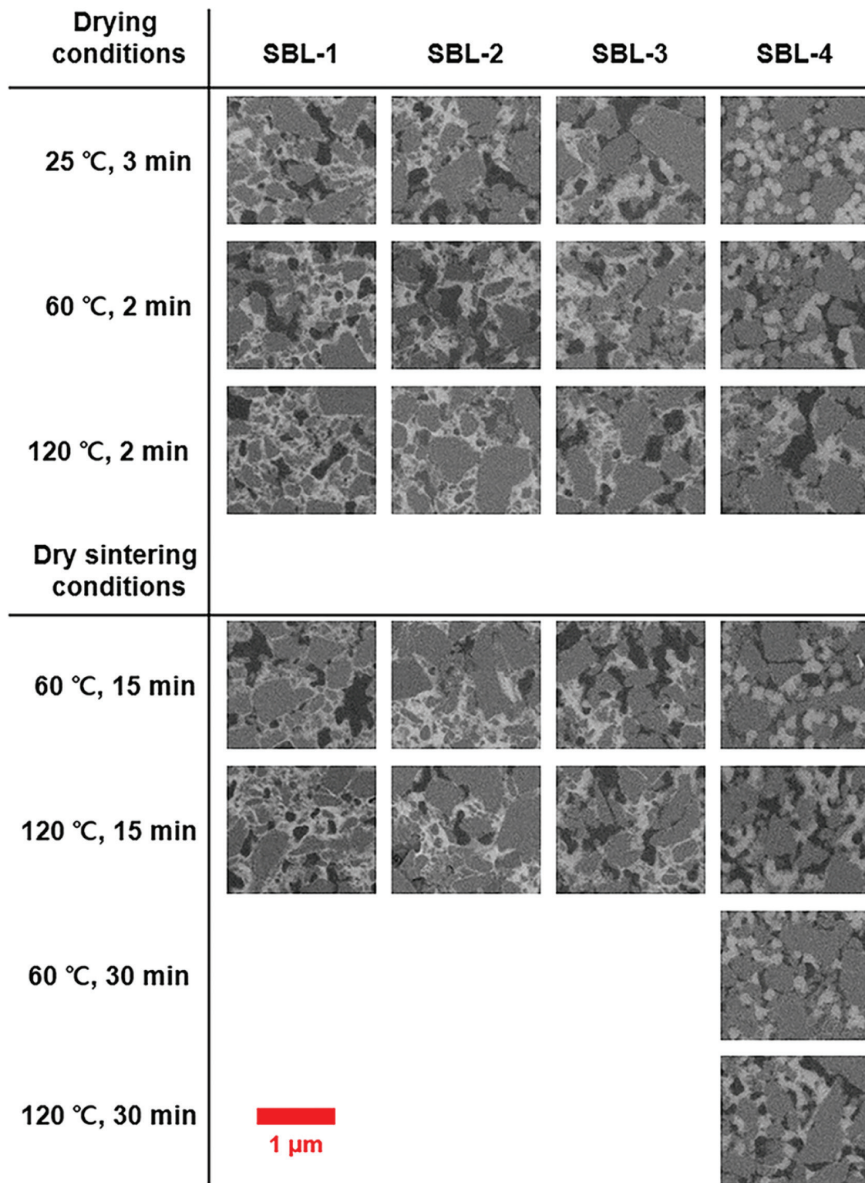


**Figure 6.** Representative coating layer images showing the morphological change of latex binder.

Figure 7 shows the results of proposed two parameters: S.A. index and A.A. index. S.A. index indicates the state of dispersion and spreading of the latex binder at a given binder dosage, and A.A. index represents the amount of physical adhesion of the latex binder to the pigments at a given binder dosage. Overall, these

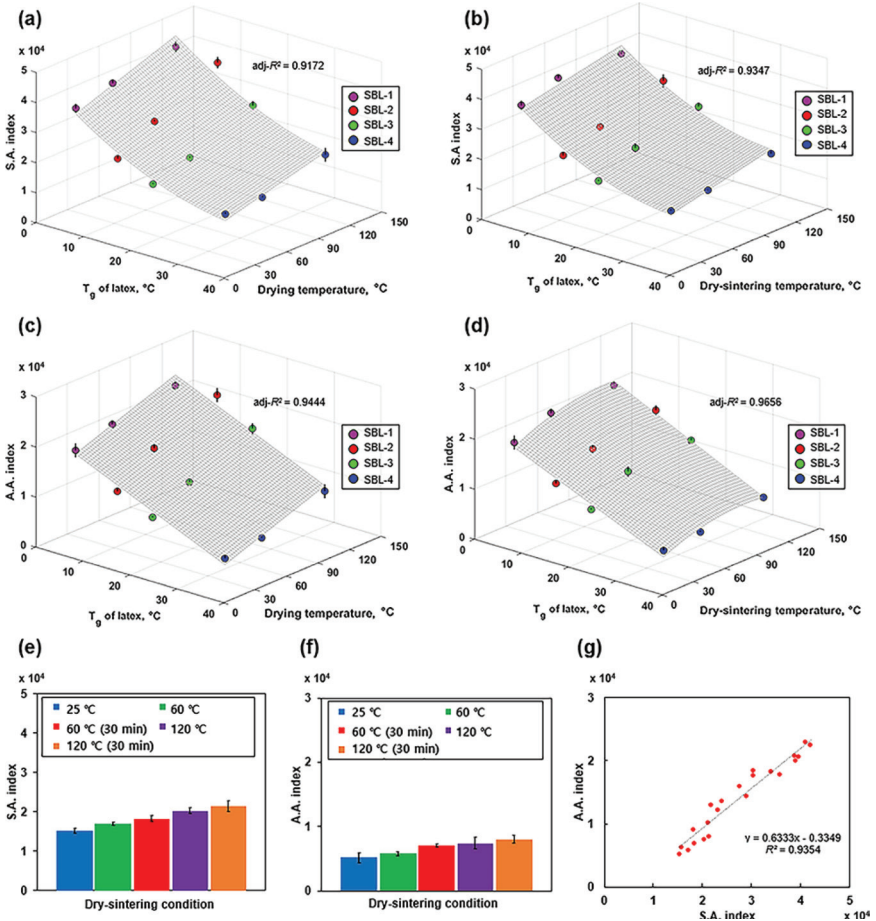


**Figure 7.** Results of proposed two parameters. Dependence of S.A. indexes on the  $T_g$  of latex and (a) drying temperature and (b) dry-sintering temperature. Dependence of A.A. indexes on the  $T_g$  of the binder and (c) drying temperature, and (d) dry-sintering temperature. Curves were fitted to describe the trends of the results in three-dimensional (3D) graphs, using the curve-fitting tool in MATLAB. Curves were generated using polynomial fitting to give the highest adjusted  $R^2$  values. Influence of the duration of dry-sintering process on the (e) S.A. index and (f) A.A. index. (g) Correlation between the S.A. index and A.A. index.

two novel parameters effectively distinguished the morphological differences of the binder. Both indices monotonically increased when the  $T_g$  of latex binder decreased or when the processing temperature increased. The increase of both indices was smaller when dry-sintering was employed. These results imply that the rubbery state of the binder particles in a wet coating color during drying significantly influences the spreading and adhesion behavior of the latex binder. The high correlation between the two indices showed that when the surface area of the latex binder increased, the adhesion between the binder and the pigment increased.

### 3.2. Coating structure development with varying spreading extent of latex

Figure 8 shows the results of adhesion ratio and its correlation with the S.A. index. The ratio was substantially low when SBL-4 latex was used, and there was only a marginal difference between the coating layers composed of other latexes. When the adhesion ratio was plotted against the S.A. index, there was a dramatic increase

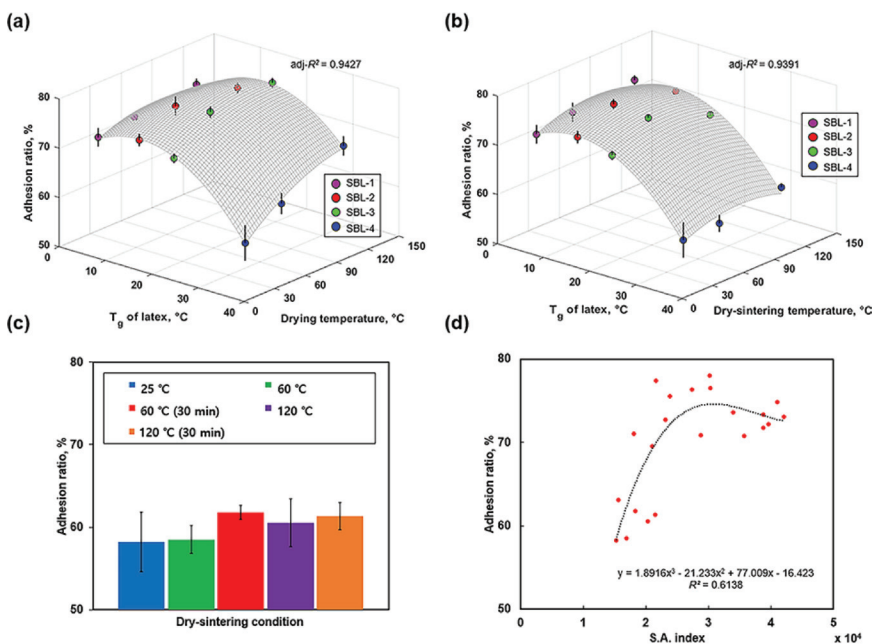


**Figure 8.** Results of the adhesion ratio and its correlation with the S.A. index. Dependence of the adhesion ratio on the  $T_g$  of the latex binder and (a) drying temperature and (b) dry-sintering temperature. (c) Influence of the duration of the dry-sintering process on the adhesion ratio. (d) Correlation between the adhesion ratio and S.A. index.

when the S.A. index was lower than  $2.2 \times 10^4$ . This was followed by a marginal change, and in some cases, even a slight reversal was observed in the domain of high latex spreading. These results indicate that small increases in the latex spreading will significantly contribute to the adhesion of the binder in the region where the S.A. index is lower than  $2.2 \times 10^4$ .

This transitional change was also observed in the distribution of pigment–binder interface length and pore size distribution (Figure 9). Indeed, they showed a close correlation with the adhesion ratio (Figure 10). One notable point was that the pore size increased slightly in the high latex spreading domain, while the adhesion ratio and the length distribution of the pigment–binder interface decreased slightly in the same domain.

This transitional change in the coating structure can be explained as depicted in Figure 11. It was hypothesized that the influence of the deformation of binder particles on the adhesion behavior greatly depends on the morphological state of the binder particles. Consider, for example, spherical latex particles that are not deformed (Figure 11b). Such latex particles have less adhesive interaction to the pigment particles, and tend to behave like small pigment particles. Thus, they fill the large pores to create a number of small pores between the particles. These latex particles will have discrete points of adhesion rather than continuous adhesion area. In this case, the surface area of the binder will be close to the total surface area of the spherical latex particles. A small increase in latex spreading will dramatically change the adhesion pattern (Figure 11c). The small pigment–binder interface formed by the discrete adhesion points would be changed into large pigment–binder interfaces. The increased deformability of the latex will eliminate the small interstices between particles and creates large pores. This can be attributed to the preferential filling of small pores induced by the capillary force [24–26]. Beyond a certain degree of spreading, further deformation would cause only a marginal increase in the coverage of the pigment by binder.

The hypothesis described above agrees well with the observation made in this study. In the case of the SBL-4 coating layer dried at 25 °C, only marginal spreading of the latex particle was observed because its MFFT was higher than the drying temperature. Indeed, the coating layer image in Figure 6 shows that the SBL-4 particles maintained the spherical shape. Therefore, the increase in the drying temperature had a significant effect on the length distribution of pigment–binder interfaces and pore size distribution for the coating layers with SBL-4. Dry-sintering showed less effects on the spreading and adhesion behavior of the latex binder, because it precluded the movement of latex particles by capillary pressure during the consolidation process, and because the dried latex particles deformed less than the wet latex particles [5, 7]. The increased coverage of small pigment particles in the high latex spreading domain creates short pigment–binder interfaces, leading to a slight decrease in the length distribution of the pigment–binder

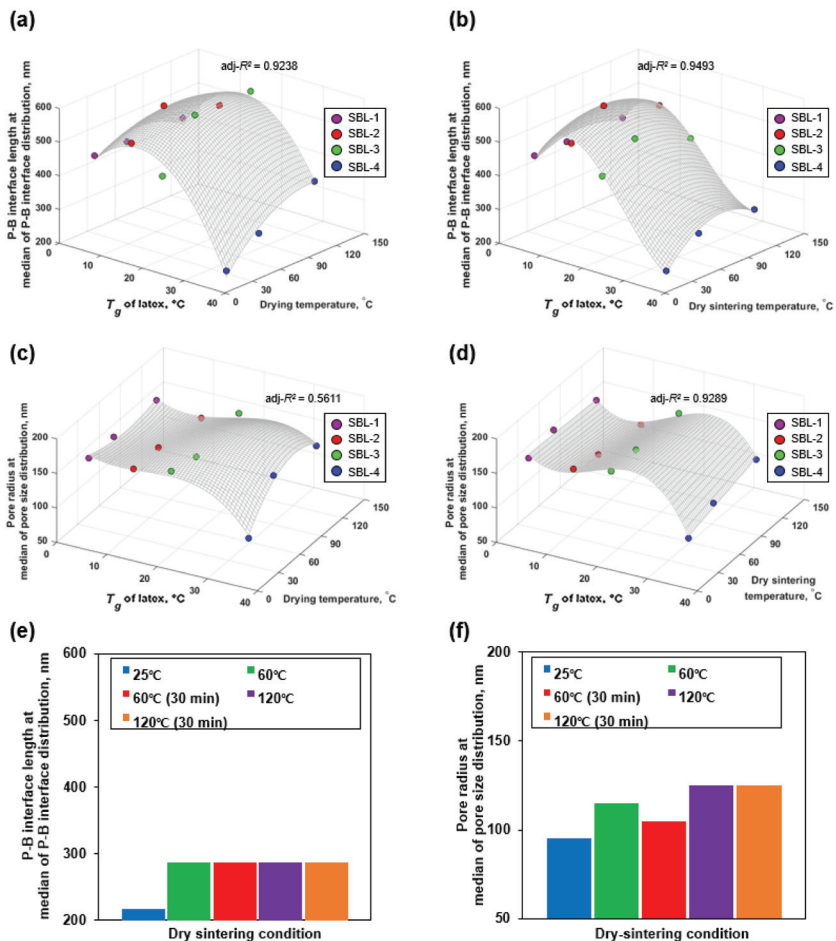


**Figure 9.** Length distribution of pigment–binder (P–B) interfaces and pore size distribution. P–B interface length at the median of P–B interface distribution with different  $T_g$  latexes and (a) drying temperature, and (b) dry-sintering temperature. Pore radius at the median of the pore size distribution with different  $T_g$  latexes and (c) drying temperature and (d) dry-sintering temperature. (e) Influence of the duration of dry-sintering process on distribution of lengths of P–B interfaces. (f) Influence of the duration of dry-sintering process on pore size distribution.

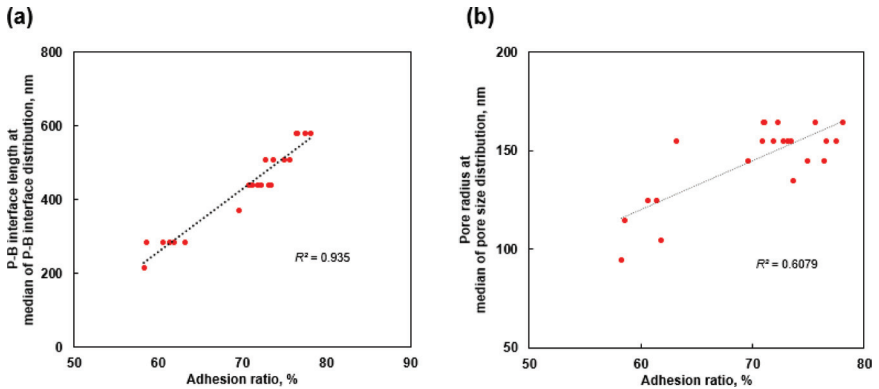


**Figure 10.** Correlation between adhesion ratio and (a) length distribution of pigment–binder (P–B) interfaces and (b) pore size distribution.

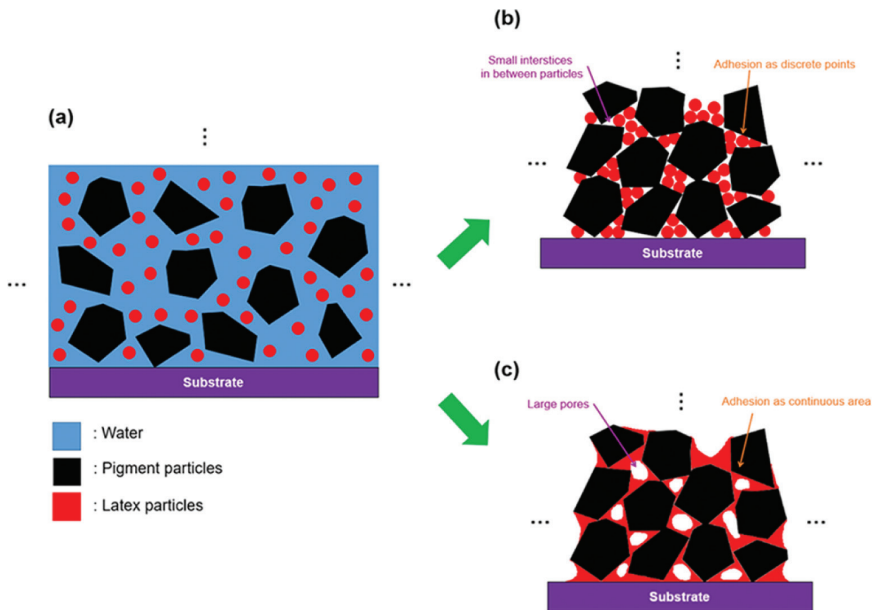


**Figure 11.** Scheme of the transition of the adhesion behavior of latex particles. (a) Particles dispersed in wet coating color. (b) Dry coating structure, when latex particles have spherical shape. (c) Dry coating structure when latex particles are deformed. Significant changes in the arrangement of latex particles and adhesion pattern occurred when the morphological state of the latex changed from (b) to (c). Note that this scheme assumes that the arrangement of pigment particles is fixed and the size of pigment particles are almost similar, which is different from the actual consolidation process.

interface. However, this eliminates the small interstices between the particles, leading to a slight increase of the pore size distribution.

### 3.3 Correlation between the end-use properties and the structure of coating layers

The observed transitional change in the coating structure described in 3.2 had a significant influence on the end-use properties of the coating layers (Figure 12, 13). The mechanical strength of the coating layers increased as the latex spreading increased (Figure 12). This was attributed to an increase in the coverage of the pigment particles by the binder. The increase was more significant in the low latex spreading domain, which corresponded to the transitional change of the coating structure. This implies that the change in adhesion pattern had a significant influence on the development of mechanical strength. Another interesting result was that the peel strength value rarely increased after reaching 117 N/m. It was speculated that the deformation of latex beyond a certain level of latex spreading mainly

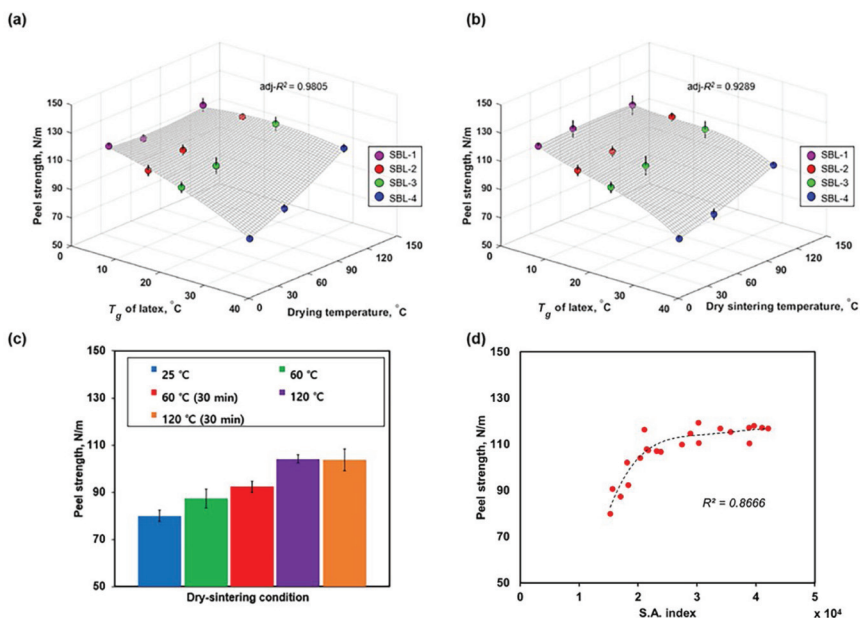


**Figure 12.** Results of mechanical property measurement and its correlation with the latex spreading. Peel strength as a function of  $T_g$  of latex and (a) drying temperature and (b) dry-sintering temperature. (c) Influence of the duration of dry-sintering process on the peel strength of coating layers. (d) Correlation between peel strength and S.A. index.

contributed to an increase in the coverage of smaller pigment particles by the binder or an increase in the pigment–pore interfaces, with little enhancement on the adhesion between the pigment particles.

The result of light-scattering efficiency was also consistent with the transitional change of the coating structure, showing a high correlation with the pore size distribution (Figure 13). The optimal average pore size for light scattering of the GCC coating layer is  $0.2\ \mu\text{m}$  [27]. The average pore size of the coatings used in this study was smaller than that (Figure 13d), which was the reason why the light scattering efficiency was proportional to the pore size distribution.

The micro-roughness of the coating surface was highly correlated with the latex spreading (Figure 14), while PPS roughness had no correlation with it (Figure 15). The PPS roughness values of all coating layers were approximately  $0.80\ \mu\text{m}$ , which was the same as that of the base substrate. This indicates that the large-scale roughness is highly dependent on the unevenness of the substrate. A

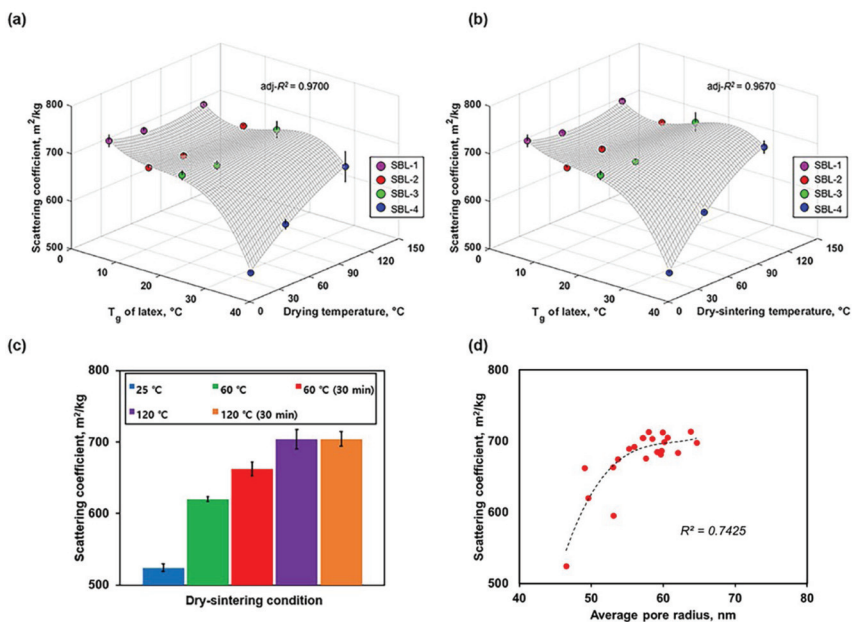


**Figure 13.** Light-scattering efficiency of coating layers and its relation to pore size distribution. Light-scattering coefficient of coating layers as a function of  $T_g$  of latex and (a) drying temperature and (b) dry-sintering temperature. (c) Influence of the duration of dry-sintering process on the light-scattering efficiency. (d) Correlation between the average pore radius and light-scattering coefficient.

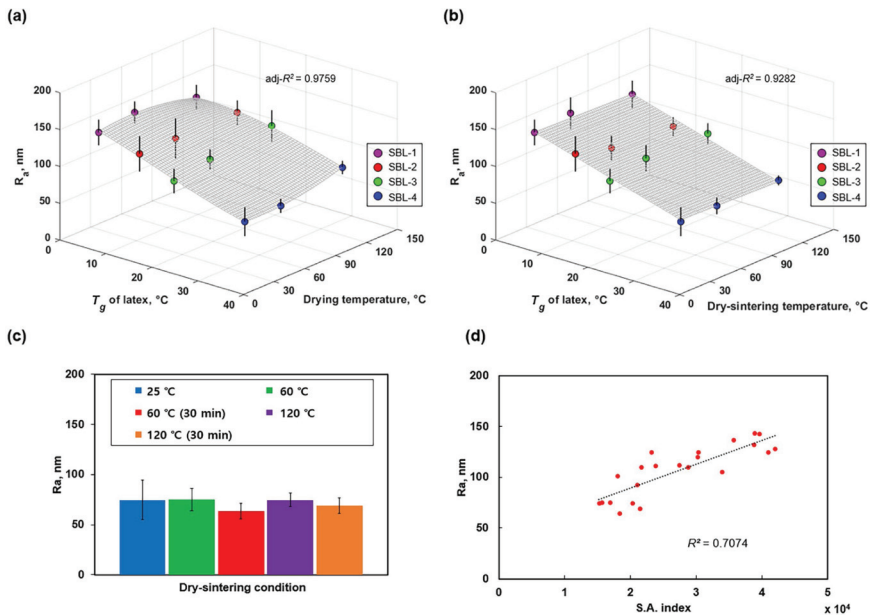


**Figure 14.** Micro-roughness of coating surface and its relation to spreading of latex. Dependence of the arithmetic mean roughness on  $T_g$  of latex and (a) drying temperature and (b) dry-sintering temperature. (c) Influence of duration of dry-sintering process on micro-roughness. (d) Correlation between S.A. index and arithmetic mean roughness.

high correlation was observed between the micro-roughness and the gloss of the coating layer (Figure 15). It was notable that the micro-roughness and gloss of the coating layer changed beyond the transitional change observed in this study.

The correlation between the structural properties of the coating layer and the end-use properties provided an interesting point of discussion. It has been reported that various end-use properties showed transitional changes depending on the deformability of the latex binder [8-9, 28-30]. Lee [28-29] observed a step change in coating gloss with S/B ratio or drying temperature, and he termed it as “gloss transition”. This gloss transition was understood in terms of coating shrinkage induced by the deformability of the latex, which was supported by SEM imaging of the coating surface [29] and measurement of the storage modulus of the S/B latex [30]. The observations made in this study indicated that this gloss transition can be divided into two regions. In the first region, abrupt changes in the coating structure and properties occurred, corresponding to the transitional change observed in this study. In the second region, gradual changes in several coating properties such as surface smoothness and gloss occurred.

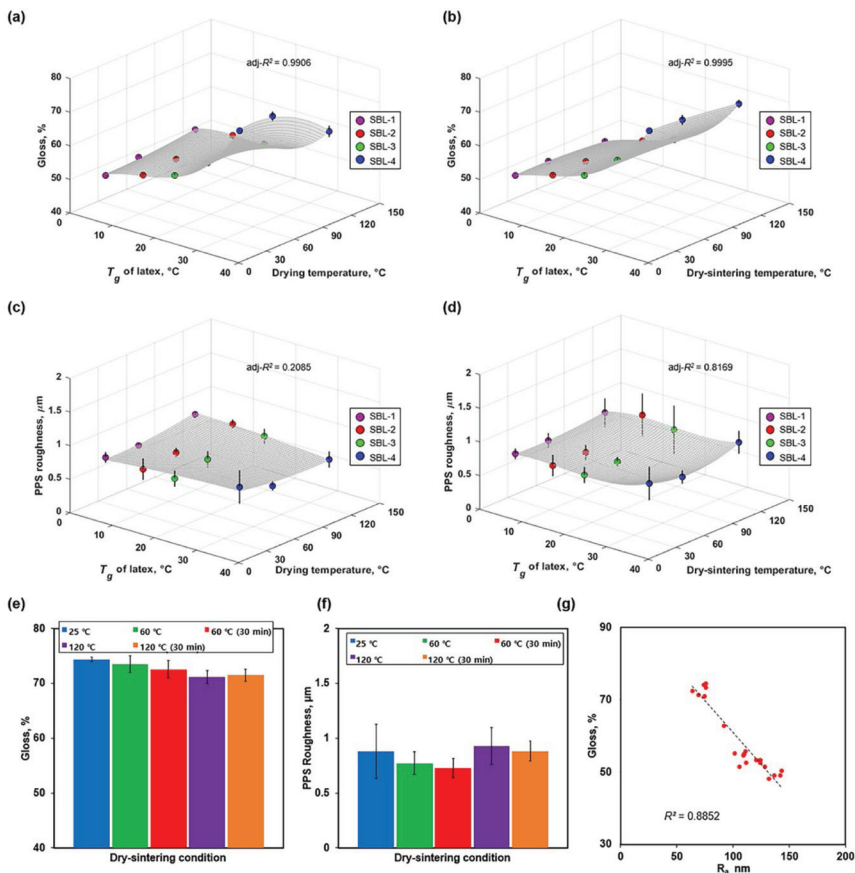


**Figure 15.** Results of gloss and PPS roughness of coating layers. Gloss of the coating layer as a function of  $T_g$  of latex and (a) drying temperature and (b) dry-sintering temperature. PPS roughness of the coating layer as a function of  $T_g$  of latex and (c) drying temperature and (d) dry-sintering temperature. Influence of duration of dry-sintering process on (e) gloss and (f) PPS roughness. (g) Correlation between gloss and arithmetic mean roughness ( $R_a$ ).

Another interesting observation was that the micro-roughness changed while there was little shrinkage of the coatings. Because the latex content of the coating layer used in this study was low, there was little change in the dimension of the coating layer [31-32] (Figure 16). The spreading of the latex binder affected the coating surface morphology aside from coating shrinkage.

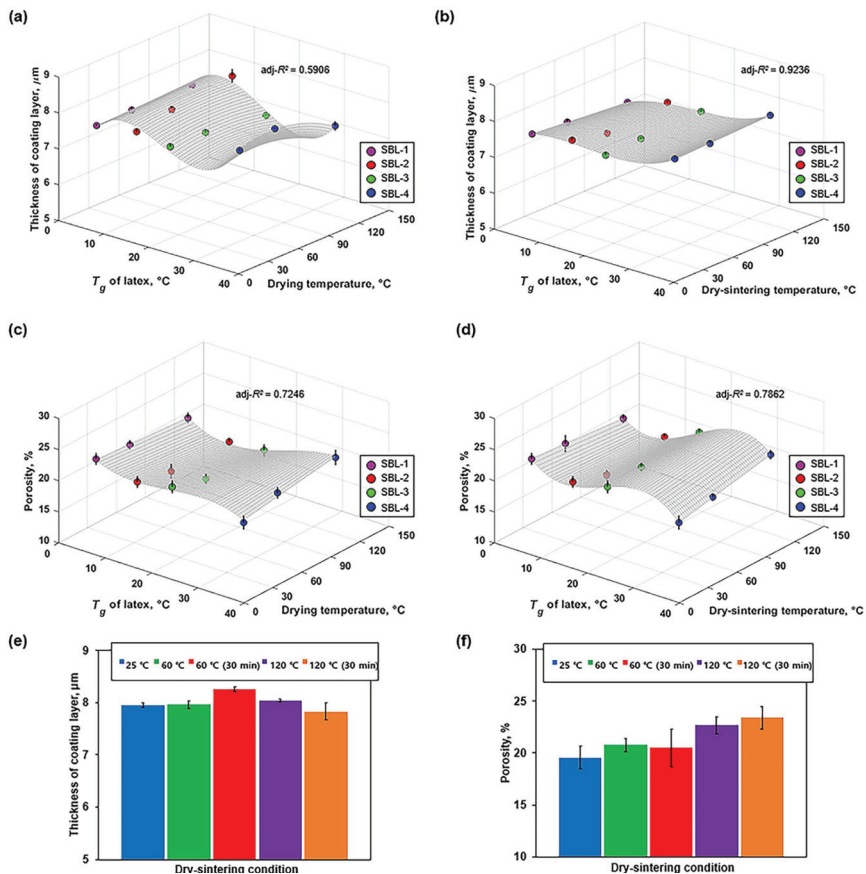


**Figure 16.** Results of the thickness and porosity of the coating layer. Thickness of coating layer depending on  $T_g$  of latex and (a) drying temperature and (b) dry-sintering temperature. Porosity of the coating layer depending on  $T_g$  of latex and (c) drying temperature and (d) dry-sintering temperature. Influence of duration of dry-sintering process on (e) thickness and (f) porosity of coating layer.

### 3.4 Separation of physical and chemical aspects of the adhesion behavior of latex binder

Quantitative analysis of the correlation between the spreading of latex and the mechanical properties of the coating layer allowed us to separate the adhesion behavior of latex binders into physical and chemical aspects. The results showed that the degree of latex spreading required to achieve a certain mechanical strength

depended on the  $T_g$  of latex (Figure 17). A linear relationship was observed when the correlation between the peel strength of the coating layer and the S.A. index was plotted according to the type of latex. The gradient of this relationship increased as the  $T_g$  of the latex increased. This showed that when a higher  $T_g$  latex was used, a lesser degree of latex spreading was required to achieve the upper limit of peel strength. It is known that for pure latex or pigmented latex films, an S/B copolymer latex with a higher styrene ratio yields higher mechanical strength [33-34]. The results of this study suggested that the chemical composition of S/B latex also affected the adhesion between the latex binder and pigment particles.

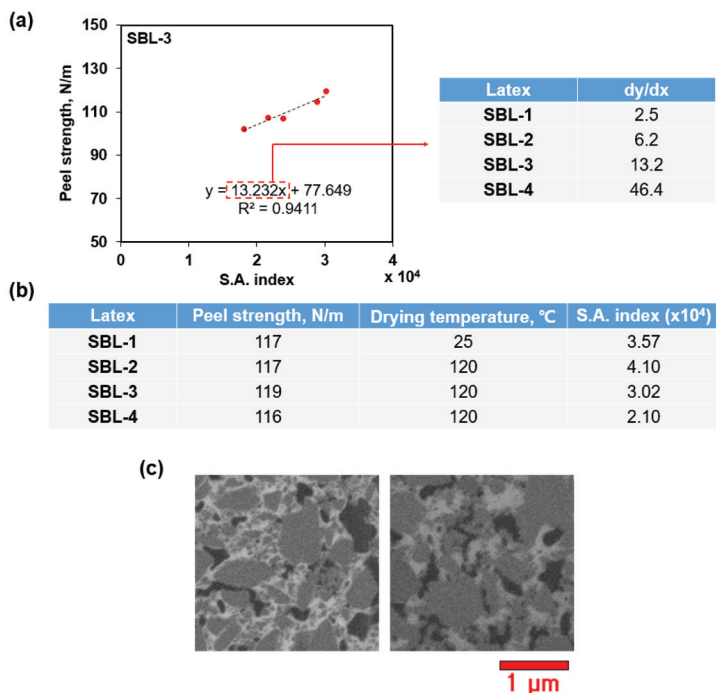


**Figure 17.** Influence of the chemical composition of S/B latex on the mechanical property of coating layers. (a) Gradient of linear regression line between peel strength and S.A. index, (b) spreading extent of latex (S.A. index) of four different S/B latexes which reached an upper limit of peel strength. (c) Coating layer images with an upper limit of peel strength. Note a substantial difference in S.A. index between two coatings, namely, those containing SBL-1 latex dried at 25 °C (left) and SBL-4 latex dried at 120 °C (right).

The use of high- $T_g$  latex will allow fabricating stronger coating layers with minimal spreading of the latex. This would be beneficial in achieving other desirable properties such as gloss. However, the drying conditions must be controlled to obtain desirable mechanical properties, and this increases the drying cost. However, the results suggested one strategy for optimizing the properties of coated paper products.

## **4 CONCLUSION**

New parameters and techniques have been developed for quantitative analysis of the spreading and adhesion behavior of latex binders. This new approach effectively distinguished the morphological changes of the latex binder in the coating layers compared to the qualitative observations using the SEM images. Analytical techniques developed were applied to analyze various correlations between the structural properties and the end-use properties of coating layers prepared to have varying extents of latex spreading. The finding contributed to better understanding of the development of coating structures affected by the deformation of latex binders. The conclusion is as follows:

- Transitional changes in the coating structure and properties was observed in the low latex spreading domain. This dramatic change was attributed to the change in the adhesion pattern of the latex binder from discrete point adhesion to continuous adhesion, and to the preferential filling of small pores that increased the pore size.
- Micro-roughness and gloss of the coating surface showed a strong correlation with the latex spreading, but there was little change in the dimensions of the coating layer due to the low latex content. This provided the observation that the spreading of latex binder affected the surface morphology of the coating in addition to coating shrinkage.
- Latex with higher styrene ratio gave a stronger coating layer with minimal spreading. This result suggested a strategy for manufacturers to produce coated paper products with better end-use properties.

## **ACKNOWLEDGEMENTS**

The authors thank to LG. Chem for providing valuable support and comments. This study was supported by National Research Foundation of Korea (NRF) grant funded by the Korean government (No. 2019R1H1A2080316, No. 2020R1A2C1014812, and No. 2018R1A5A1024127)

## REFERENCES

- [1] R. Groves, G. P. Matthews, J. Heap, M.D. McInnes, J.E. Penson and C.J. Ridgway. Binder migration in paper coatings—a new perspective. In **The Science of Paper-making**, *Trans. 12th Fund. Res. Symp.*, (ed. C.F. Baker), pp1149–1181, FRC, Manchester, 2001.
- [2] G. Engström and M. Rigdahl. Binder migration—effect on printability and print quality. Literature review. *Nord. Pulp Pap. Res. J.* **7**(2):55–74, 1992.
- [3] K. Yamazaki, T. Nishioka, Y. Hattori and K. Fujita. Print mottle effect of binder migration and latex film formation during coating consolidation. *Tappi J.* **76**(5):79–84, 1993.
- [4] M. Ragnarsson. Variations related to print mottle in starch-containing paper coatings, PhD Thesis, Department of Chemical Engineering, Karlstads Universitet, Karlstad, 2012.
- [5] J. Watanabe and P. Lepoutre. A mechanism for the consolidation of the structure of clay-latex coatings. *J. Appl. Polym. Sci.* **27**(1): 4207–4219 (1982).
- [6] J. Järnström, M. Väisänen, R. Lehto, A. Jäsberg, J. Timonen and J. Peltonen. Effect of latex on surface structure and wetting of pigment coatings. *Colloids Surf. A Physicochem. Eng. Asp.* **353**(2–3):104–116 (2010).
- [7] P. Wedin, C.J. Martinez, J.A. Lewis, J. Daicic and L. Bergström. Stress development during drying of calcium carbonate suspensions containing carboxymethylcellulose and latex particles. *J. Colloid Interface Sci.* **272**(1):1–9 (2004).
- [8] D.I. Lee. Latex applications in paper coating, in **Polymeric Dispersions: Principles and Applications** (ed. J.M. Asua), Kluwer Academic Publishers, Dordrecht, 1997.
- [9] D.A. Taber and R.C. Sten. Effect of latex variables on properties of coating colors and coated papers. *Tappi J.* **40**(2): 107–117 (1957).
- [10] R.D. Purfeerst and R.L. Van Gilder. Tail-edge picking, back-trap mottle and fountain solution interference of model latex coatings on a six-color press predicted by laboratory tests. In *proc. Tappi 1991 Coating Conference*, pp461–472, Montreal, Quebec, 1991, Tappi Press, Atlanta, 1991.
- [11] P. Ihalainen, K. Backfolk, P. Sirviö and J. Peltonen. Topographical, chemical, thermal and electrostatic properties of latex films. *Colloids Surf. A. Physicocheml Eng Asp.* **354**(1–3):320–330 (2010).
- [12] V. Granier and A. Sartre. Ordering and adhesion of latex particles on model inorganic surfaces. *Langmuir.* **11**(6):2179–2186 (1995).
- [13] W.N. Unertl. Wetting and spreading of styrene-butadiene latexes on calcite. *Langmuir.* **14**(8):2201–2207 (1998).
- [14] J.K. Dreyer, T. Nylander, O.J. Karlsson and L. Piculell. Spreading dynamics of a functionalized polymer latex. *ACS Appl. Mater. Interfaces.* **3**(2):167–176 (2011).
- [15] M. Reitsma, V.S. Craig and S. Biggs. Measurement of the adhesion of a viscoelastic sphere to a flat non-compliant substrate. *J. Adhes.* **74**(1–4):125–142 (2000).
- [16] L.P. DeMejo, D.S. Rimai and R.C. Bowen. Direct observations of deformations resulting from particle-substrate adhesion. *J. Adhes. Sci. Technol.* **2**(1):331–337 (1988).

- [17] M. Joanicot, V. Granier and K. Wong. Structure of polymer within the coating: an atomic force microscopy and small angle neutrons scattering study. *Prog. Org. Coat.* **32**(1–4): 109–118 (1997).
- [18] J.H. Lee, K. Oh, A.R. Abhari and H.L. Lee. Characterization of paper coating structure using FIB and FE-SEM. 1. new method for image analysis. *Ind. Eng. Chem. Res.* **57**(12):4237–4244 (2018).
- [19] J.H. Lee and H.L. Lee. Characterization of the paper coating structure Using focused ion beam and field-emission scanning electron microscopy. 2. Structural variation depending on the glass transition temperature of an S/B Latex. *Ind. Eng. Chem. Res.* **57**(49):16718–16726 (2018).
- [20] P. Alam, M. Toivakka, E. Lazarus and P. Salminen. On the mechanism of wet and dry strength of paper coatings: part 2 – modeling and simulation. In proc. *Tappi 2012 PaperCon*, pp550–556, New Orleans, USA, Tappi Press, Atlanta, 2012.
- [21] M. Toivakka, P. Alam, F. Touaiti, A. Oravilhti, T. Oravilhti, J. Knuutinen, R. Nilsson, M. Pahlevan, M. Ahokas and C. Wilen, Understanding coating strength at the molecular and microscopic level. *Tappi J.* **14**(6):373–383 (2015).
- [22] S.M.H. Najafi, D.W. Bousfield and M. Tajvidi, Evaluation of the adhesion performance of latex-starch mixtures to calcium carbonate surfaces. *Nord. Pulp Pap. Res. J.* **34**(3):318–325 (2019).
- [23] J.H. Lee and H. L. Lee, Novel method for the evaluation of mechanical property of pigment coating layer and its application: Influence of spreading of latex binder on final properties of coating layer. *Prog. Org. Coat.* **163**:106652 (2022).
- [24] C. Kugge. An AFM study of local film formation of latex in paper coatings. *J. Pulp Pap. Sci.* **30**(4):105–111 (2004).
- [25] C. Dahlström. Quantitative microscopy of coating uniformity, PhD thesis, Department of Applied Science and Design, Mid Sweden University, Sundsvall, 2012.
- [26] G. Ström, J. Hornatowska, X. Changhong and O. Terasaki. A novel SEM cross-section analysis of paper coating for separation of latex from void volume. *Nord. Pulp Pap. Res. J.* **25**(1):107–113 (2010).
- [27] P.A.C. Gane, L. Huggenberger, M. Arnold and H. Köster. Pigments. Ch 5. in **Paper-making Science and Technology: Book 11. Pigment coating and surface sizing of paper** (ed. J. Paltakari), Paperi ja Puu Oy, Helsinki, 2009.
- [28] D.I. Lee. Development of high-gloss paper coating latexes. In proc. *Tappi 1982 Coating Conference*, pp125–135, San Francisco, California, USA, Tappi Press, Atlanta, 1982.
- [29] D.I. Lee. A fundamental study on coating gloss. In proc. *Tappi 1974 Coating Conference*, pp97–114, Tappi Press, Atlanta, 1974.
- [30] R. Groves, J.E. Penson and C. Ruggles. Styrene-butadiene latex binders and coating structure. *Tappi 1993 Coating Conference*, pp187–205, Minneapolis, Minnesota, USA, 1993.
- [31] A. Stanislawska and P. Lepoutre. Consolidation of pigmented coatings: development of porous structure, *Tappi J.* **79**(5):117–125 (1996).
- [32] P. Lepoutre and B. Alinec, Dry sintering of latex particles in pigmented coatings. I. Influence on coating structure and properties, *J. Appl. Polym. Sci.* **26**(3):791–798 (1981).

- [33] M. Parpaillon, G. Engström, I. Pettersson, I. Fineman, S.E. Svanson, B. Dellenfalk and M. Rigdahl. Mechanical properties of clay coating films containing styrene–butadiene copolymers. *J. Appl. Polym. Sci.* **30**(2):581–592 (1985).
- [34] J. Zhao and G.N. Ghebremeskel, A review of some of the factors affecting fracture and fatigue in SBR and BR vulcanizates. *Rubber Chem. Technol.* **74**(3):409–427 (2001).

## Transcription of Discussion

# QUANTITATIVE ANALYSIS OF THE SPREADING AND ADHESION OF LATEX BINDER WITHIN PIGMENT COATING LAYER AND ITS RELATION TO THE END-USE PROPERTIES OF THE COATING LAYER

*Jee-Hong Lee*<sup>1,2</sup>, *Sang Jin Shin*<sup>5</sup>, *Seung Uk Yeu*<sup>5</sup> and  
*Hak Lae Lee*<sup>2,3,4</sup>

<sup>1</sup> Center for Coating Materials and Processing, Seoul National University.

<sup>2</sup> Department of Agriculture, Forestry and Bioresources, College of Agriculture and Life Sciences, Seoul National University, South Korea.

<sup>3</sup> Research Institute of Agriculture and Life Sciences, Seoul National University.

<sup>4</sup> State Key Laboratory of Biobased Material and Green Papermaking, Qilu University of Technology (Shandong Academy of Sciences), Jinan, 250353, the People's Republic of China.

<sup>5</sup> Petrochemicals R&D, Research Park, LG Chem. Limited., 34122 Daejeon, South Korea.

*Janet Preston*      Imerys Minerals Ltd

You have developed some really interesting techniques which could be really useful for a number of different areas in paper. You suggested that you have used these methods in other work, so please could you expand a bit more on where they could possibly be used?

## *Discussion*

*Jee-Hong Lee*

Okay, so, let me explain more details and my related experience. These approaches can be used in various types of coating or thin layers. Among the approaches introduced, I will concentrate on the approach that I used in the measurement of the latex spreading and adhesion, and comparing these to mechanical properties. This approach can be applied to the studies where the interfacial phenomenon is important. For example, this can provide valuable insights in analysing the double coatings or the slide coatings. Also, the example I'm showing on the slide is where I applied the introduced approach to the lithium ion battery electrode. Surprisingly, the structure of lithium ion battery electrode is quite similar to that of a paper coating. The active material is used instead of the pigment, but the same binders are used in an aqueous binder system, and the binder content is low. The problem that frequently occurs in the battery electrode is the delamination of the electrode layer from the substrate. I have applied the introduced approach to analyse the structure of electrode layer and related it to the delamination behaviour of the electrode. This has produced some successful results and I think that the approaches can find valuable applications in these kinds of examples.

*Peter De Clerck*      PaperTec Solutions Pte Ltd

I have a question regarding gloss in your presentation. How did you develop gloss in your paper before making the measurement? Was it thermal treatment, mechanical treatment or was it just levelling by surface tension of the coating mix?

*Jee-Hong Lee*

I used hot-air drying in coating layer samples. Also, some samples are exposed to dry-sintering after drying, so I can say that I used some thermal approaches in developing the gloss.

*Peter De Clerck*

So, no mechanical or thermal treatment basically to rearrange the pigment on the surfaces of the paper, it was only surface tension levelling . . . natural drying?

*Jee-Hong Lee*

Yes, just drying.

*Peter De Clerck*

You reported a very significant impact on the gloss. Rearrangement of the coating pigments is absolutely critical for gloss development. The more adhesion between the pigments, the more difficult it is to rearrange them and the more difficult it is to develop gloss within the paper. This did not seem to be considered in your work.

*Steve Keller*      Miami University

Did you see any difference in the particle size distribution of the particles shown in each of the individual images?

*Jee-Hong Lee*

Was this in case of pigment particles?

*Steve Keller*

Yes, the pigment particles shown in the 22 images illustrated in the report. Did you see any differences in the particle size distribution in those images?

*Jee-Hong Lee*

I did not measure the characteristics of pigment particles in this study, but I am quite sure that this is similar because I used the same material. I mean, we used the same GCC.

*Steve Keller*

What I am driving at is, it appeared that you observed smaller spaces in those images that might not be fully representative of the overall system. I am not really concerned about the particle size distribution per se, but rather I am concerned that the larger particles present in some images might have acted as a heat sink that will change the observed thermal response of the latex particles that are in contact. If you had images with larger particle sizes, would that show less melting of the latex particles?

*Jee-Hong Lee*

So, you are worrying about the representativeness of the coating images. If I understood right, your concern is that if there are large pigment particles, the latex spreading may occur differently? This is actually one of the skipped details in my

## *Discussion*

presentation which is related to acquiring these high-quality cross-section images. Image analysis always confronts the problem that one may point out that you may use images containing just what you want to show. So, I performed an experiment to know how many images should be acquired to validate the representativeness of coating layer images. Here is what I did. I took a bunch of cross-section images and observed the changes of the coefficient of variation of the coating porosity by adding images one by one, and repeated this in a few random orders. At first, the coefficient of variation value fluctuated as more images are added; however, this was levelled after a certain number of images. In this way, we found the least number of images required to show the representative data of coatings. The observations in this presentation are based on this method, so I can say that it is quite okay and not to worry about the representativeness of data.

*Martti Toivakka* Åbo Akademi University

My question is about binder migration. You had very large latex particles and although I do not believe in migration of large particle size latex, perhaps it can occur at the boundaries. You had one sided drying. So, did you ever look at smaller latex particles migrate or not, as there are some latexes with 50- or 60-nanometres size? There has been some discussion of that, and did you look at uniformity of your coating layers in Z or vertical direction?

*Jee-Hong Lee*

Let me answer your question with this slide. This is also one of the skipped ones. You can see that I analysed the binder distribution here. I prepared 22 coating layers, which is actually quite a large number of conditions. The reason I also tested the dry-sintering conditions was derived from the concern that the difference in distribution can be caused by drying conditions. However, after conducting the experiments, I found that there was no difference in distribution. This was constant in all coating layer samples. In case of the size, I did not try that.

*Martti Toivakka*

Did you observe more binder on the boundaries on the surface or next to the film from the wall effect?

*Jee-Hong Lee*

Surprisingly, the distribution was uniform and constant. I found similar results in some other studies. One was from this conference in the early 2000s by Robert

Groves and co-authors. They also showed that the binder migration was not observed in coatings which are comprised of only latex. They only observed the binder migration when starch was used. Well, binder migration is always a hot potato and I am not sure why coating samples in our case did not show binder migration. However, apparently, this was not observed in my experiment.

*Alexander Bismarck*      University of Vienna

You take your diamond knife and drive it through the coating and call the measured resistance peel strength, but is it not more a resistance to cutting?

*Jee-Hong Lee*

Yes. I also agree with that. This value is automatically calculated in this tool, and the developers of this tool just named this value as “peel strength”. This device is developed in Japan, so maybe the developers are not native English speakers, so they might not find appropriate naming for this: peel strength or cutting strength. I just followed what the manufacturers named.

*Alexander Bismarck*

So, you seem to have looked into the literature very thoroughly. How does it compare to a normal peel strength of a coating then?

*Jee-Hong Lee*

I also tried normal peel strength tests or some other Z-directional strength tests such as the Scott Bond Test. However, this was actually not comparable to our method because the failure also occurred between the interfaces of coating and substrate. Our method induces the failure only inside the coating layers, so the results were not comparable with that from conventional methods. It is kind of apples and oranges. I tried the conventional methods prior to our developed methods; however, it was impossible to determine where the failure occurs. And this was the reason I tried a new approach.

*Alexander Bismarck*

And also just adding to the peeling strengths?

## *Discussion*

*Jee-Hong Lee*

I just want to add one more thing about the naming of peel strength. You can see from these images that there was no direct slicing of pigments or binders by the diamond knife. The cut surface by the diamond knife still maintained the grainy surface of original coatings. And the cross-section of the failure also followed the contour of the particles well. So, I can say that this should be named after cutting; however, the situation also resembles the peeling I guess.

*Alexander Bismarck*

One more question, you said you used polymers with higher glass transition temperature which will obviously affect the mechanical properties but where in relation to  $T_g$  was the test temperature?

*Jee-Hong Lee*

The temperature was different. The reason I said this can be a strategy for optimization was because if you want to make the same latex spreading with higher  $T_g$ , you need harsher drying condition. This will increase the drying cost, and the manufacturer should compare the drying cost with the performance of the coatings.